Journal of Molecular Neuroscience (2024) 74:79
https://doi.org/10.1007/s12031-024-02256-w

RESEARCH

Electroacupuncture Alleviates Streptozotocin-Induced Diabetic Neuropathic Pain via the TRPV1-Mediated CaMKII/CREB Pathway in Rats

Yinmu Zheng[1,2] · Siyi Li[1,2] · Yurong Kang[1,2] · Qunqi Hu[1,2] · Yu Zheng[1,2] · Xiaoxiang Wang[2] · Hengyu Chi[2] · Keying Guo[2] · Minjian Jiang[1,2] · Zhouyuan Wei[1,2] · Xiaomei Shao[1,2] · Chi Xu[1,2] · Boyu Liu[1,2] · Junying Du[1,2] · Xiaofen He[1,2] · Jianqiao Fang[1,2] · Zhenzhong Lu[3] · Yongliang Jiang[1,2]

Received: 28 April 2024 / Accepted: 14 August 2024

Abstract

Diabetic neuropathic pain (DNP) is a diabetic complication that causes severe pain and deeply impacts the quality of the sufferer's daily life. Currently, contemporary clinical treatments for DNP generally exhibit a deficiency in effectiveness. Electroacupuncture (EA) is recognized as a highly effective and safe treatment for DNP with few side effects. Regrettably, the processes via which EA alleviates DNP are still poorly characterized. Transient receptor potential vanilloid 1 (TRPV1) and phosphorylated calcium/calmodulin-dependent protein kinase II (p-CaMKII) are overexpressed on spinal cord dorsal horn (SCDH) in DNP rats, and co-localization is observed between them. Capsazepine, a TRPV1 antagonist, effectively reduced nociceptive hypersensitivity and downregulated the overexpression of phosphorylated CaMKIIα in rats with DNP. Conversely, the CaMKII inhibitor KN-93 did not have any impact on TRPV1. EA alleviated heightened sensitivity to pain caused by nociceptive stimuli and downregulated the level of TRPV1, p-CaMKIIα, and phosphorylated cyclic adenosine monophosphate response element-binding protein (p-CREB) in DNP rats. Intrathecal injection of capsaicin, on the other hand, reversed the above effects of EA. These findings indicated that the CaMKII/CREB pathway on SCDH is located downstream of TRPV1 and is affected by TRPV1. EA alleviates DNP through the TRPV1-mediated CaMKII/CREB pathway.

Keywords TRPV1 · Diabetic neuropathic pain · CaMKII/CREB pathway · Capsazepine · KN-93 · Capsaicin

Introduction

Due to the increasing incidence of diabetes globally, diabetic neuropathic pain (DNP) is now a prevalent cause of neuropathic pain (Rosenberger et al. 2020). It is estimated that by 2045, one in ten individuals in the world will be living with diabetes, and of these, 60% will be affected by DNP (Magliano et al. 2021). The typical symptoms of DNP encompass nociceptive hyperalgesia, hypoalgesia, numbness, tingling, and allodynia, which cause tremendous physical along with mental suffering and affect the quality of life for DNP patients (Dan et al. 2022). Conventional treatments for DNP include opioids and NSAIDs; however, it is imperative not to overlook their adverse effects, such as addictive hazards and gastrointestinal injuries (Moran and Szallasi 2018).

Electroacupuncture (EA) is a medical treatment that links ancient Chinese acupuncture with advanced electrical stimulation. It has been well demonstrated to have a significant pain-relieving impact on various types of pain

Yinmu Zheng and Siyi Li contributed equally to this work.

Zhenzhong Lu and Yongliang Jiang is considered joint corresponding author.

✉ Zhenzhong Lu
m2mandbsb@163.com

✉ Yongliang Jiang
20111019@zcmu.edu.cn; jyl2182@126.com

[1] Key Laboratory of Acupuncture and Neurology of Zhejiang Province, Zhejiang Chinese Medical University, Hangzhou, China

[2] The Third Clinical Medical College, Zhejiang Chinese Medical University, Hangzhou, China

[3] Jinhua Wenrong Hospital, Jinhua, China

Published online: 20 August 2024

in clinical settings (Lam et al. 2022; Zhang et al. 2022b). Nevertheless, despite continuous investigation into how EA mitigates DNP, the precise molecular mechanisms remain incompletely understood.

Transient receptor potential vanilloid 1 (TRPV1) could be activated by heat, capsaicin, or inflammatory mediators (Iftinca et al. 2021), resulting in a pain response. Calcium/calmodulin-dependent protein kinase II (CaMKII) is a serine/threonine kinase activated by elevated levels of intracellular calcium ions and calmodulin (Taher et al. 2023). It was shown that TRPV1-induced calcium inward flow promotes CaMKII phosphorylation (Lv et al. 2021). Cyclic adenosine monophosphate response element-binding protein (CREB) is a major downstream target of CaMKII. Blockade of the CaMKII/CREB pathway attenuates neuropathic pain by reducing calcium in-flow (Zhang et al. 2022a). Based on the above, we hypothesize a correlation between TRPV1 and the CaMKII/CREB pathway, intending to identify novel targets for mitigating DNP.

This work was to examine the correlation of TRPV1 and CaMKII/CREB pathways in the spinal cord dorsal horn (SCDH). The activation of TRPV1 and the CaMKII/CREB pathway in SCDH of rats with DNP was examined, along with the impact of EA intervention. In that case, capsaicin was employed pharmaceutically to confirm our idea. This study provides new evidence supporting that EA alleviates DNP through the TRPV1-mediated CaMKII/CREB pathway, which offers a fresh perspective for investigating the mechanisms by which EA attenuates DNP.

Materials and Methods

Animals

Healthy male Sprague–Dawley rats (180 ~ 250 g) were purchased from Shanghai Laboratory Animal Center of China (SCXK 2017–0005). The animals were kept in the qualified Zhejiang Chinese Medical University Laboratory Animal Center (SYXK 2018–0012) (3 animals/cage, 12-h alternating cycles of light-darkness, thermostatic and humidity-controlled). All experimental animals were given unrestricted access to standardized food and drinking water at will. Each rat underwent at least 7 days of acclimatization prior to the formal conduct of the experiment. The experimental procedures were conducted in compliance with relevant guidelines and regulations as well as being reported following ARRIVE guidelines.

In total, 112 rats have been utilized. A total of 82 rats were established as DNP model rats. Then, 14 days after streptozotocin (STZ) injection, 7 rats were excluded due to failure to meet DNP criteria based on body weight (BW), fasting blood glucose (FBG), or paw withdrawal threshold (PWT). The success rate of DNP modeling was approximately 91%. Four individuals perished as a result of an intrathecal medication injection. One rat was withdrawn from the experiment midway due to an injury on its hind paw caused by a fight between caged rats, which prevented the assessment of its pain threshold. All animals were randomly grouped based on a computer-generated random order.

Establishment of DNP Model

To induce a DNP model, rats were initially fasted for 16 h. STZ (Sigma, USA) was dissolved in 0.1 mol/L of citric acid-sodium citrate buffer pH 4.5. It was then administered intraperitoneally at a dosage of 65 mg per kilogram. Successful DNP models were deemed to be established when the rats exhibited an FBG level above 16.7 mmol/L (Lu et al. 2021) with 50% of their PWT less than 5 g measured by von Frey filament test (Mixcoatl-Zecuatl and Jolivalt 2011).

Diabetes-Related General Condition Measurements

The rats underwent a 6-h fasting period before their blood glucose levels were measured. Blood samples were obtained from the tail vein by pricking, and the blood bead was applied to the siphon port of a blood glucose test strip for measurement using a blood glucose meter (Roche, Germany). FBG and BW were measured and recorded once as baseline values before the STZ injection. Subsequently, weekly measurements were conducted throughout the experiment. The investigator performed the operation unaware of the groups of rats.

Behavioral Experimental Method

PWT was quantified using the Up and Down approach, employing the von Frey filament as described (Chaplan et al. 1994). The rats designated for testing were positioned on a metal grid with a Plexiglas enclosure separating each rat. After the rats were acclimatized for 30 min, the hind paws of the rats were stimulated at different levels of intensity, and the corresponding values of these intensities were documented. To avoid injury to the rats, we set 26 g of stimulation as the upper limit of measurement. The PWT was obtained prior to STZ administration, as well as on 1 week, 2 weeks, and 3 weeks after STZ application. The investigator performed the operation unaware of the groups of rats.

EA Intervention

EA intervention was consistently administered for a duration of one week in DNP + EA, DNP + EA + veh, and DNP + EA + capsaicin groups, starting on the 15th day following the injection of STZ. Prior to EA treatment, all rats were gently restrained in black sacks. Initially, two pairs of acupuncture needles measuring 0.18 mm × 13 mm were bilaterally put on of the Zusanli (ST36) and Kunlun (BL60) acupoints in rats (Zhang et al. 2002). The insertion was done at a depth of around 5 mm, specifically in the posterolateral knee region about 5 mm below the fibula head for Zusanli, and between the tip of the outer ankle and the tendon for Kunlun. The needles were connected to the electroacupuncture device (HANS, China). Previous studies by our team confirmed that applying electrical stimulation at a frequency of 2 Hz has a notable pain-relieving impact on DNP (He et al. 2017; Fei et al. 2020). Hence, we selected the EA parameters as follows: 2 Hz, 0.5–1.0 mA, 30 min per day for a 7-day period.

Drug Preparation and Application

Drug application was consistently administered for a duration of 1 week, beginning on the 15th day following STZ injection. The TRPV1 antagonist capsazepine (Sigma-Aldrich, USA) was initially prepared in DMSO and subsequently diluted in saline for injection. Capsazepine was administered as intrathecal injections at a dose of 30 μg/rat/day in DNP + capsazepine group, with each injection containing a 20 μl volume (Haranishi et al. 2021). Similarly, CaMKII inhibitor KN-93 (Sigma-Aldrich, USA) was initially dissolved in DMSO and re-dissolved in saline before use (50 nM, 0.5 ng/20 μl) (Shirahama et al. 2012) in DNP + KN-93 group. A TRPV1 agonist, capsaicin (MCE, USA) (75 ug/20 μl) (Bach and Yaksh 1995), was injected intrathecally into the DNP + EA + capsaicin group rats after each EA intervention. A control vehicle consisting of a 0.1% DMSO-saline mixture was administered to the remaining rats by injecting an equivalent volume of solution once daily over a period of 15–21 days after STZ injection.

Intrathecal Injection

As in previous studies performed operations (Mestre et al. 1994), first, exposing the skin in the area 2–3 cm above and below the iliac crest. The horizontal position of the transverse pair of the hip joint was the L5-6 spinous processes of the rat. The rat was gently pulled upward using the nondominant hand to open the space between the vertebral segments. Insert the needle into the lumbar vertebrae in the midline of the spine at an angle of 70–90°. When the tip of the needle is felt to touch the bone surface, adjust the angle of the needle and insert the needle between the vertebral segments. Gently depress the piston of the syringe and inject the medicine into the subarachnoid space.

Western Blotting

After rats were anesthetized with intraperitoneal injection of sodium pentobarbital at a dosage of 40 mg per kilogram, the L4-L6 spinal cord tissue was excised and the dorsal horn of the spinal cord was carefully separated using microscopic scissors and microtome forceps. Subsequently, the SCDH tissues were homogenized and centrifuged in RIPA lysis solution. The supernatant was collected and measured by the BCA technique. The SCDH proteins were separated by electrophoresis and transferred onto PVDF membranes. The membranes were incubated in a 5% nonfat milk solution for 1 h at room temperature. Following blocking, primary antibodies were incubated for 16 h at 4 °C, followed by incubation with secondary antibodies for 2 h at ambient temperature. The following antibodies were utilized in this experiment: rabbit anti-TRPV1 (1:1000, ACC-030, Alomone), rabbit anti-p-CamIIα (1:1000, ab5683, Abcam), mouse anti-CamIIα (1:1000, #50049 s, CST), rabbit anti-p-CREB (1:1000, #9198s, CST), rabbit anti-CREB (1:1000, ab32515, Abcam), rabbit anti-TNF-*α* (1:1000, ab66579, Abcam), anti-rabbit IgG, HRP-linked (1:5000, #7074 s, CST), and anti-mouse IgG, HRP-linked (1:5000, #7076 s, CST). Mouse anti-β-actin (1:5000, #3700 s, CST) served as the loading control in this experiment.

Immunofluorescence

L4-L6 SCDH tissues were removed from anesthetized rats by transcardial perfusion of saline followed by 4% paraformaldehyde. The rat SCDH tissues were immersed in 4% paraformaldehyde, 15% sucrose, and 30% sucrose solution sequentially for 4, 24, and 48 h, respectively. The samples were freeze-embedded in OCT and then cut into slices with a thickness of 20 μm and adhered to slides. Sections were blocked with 10% donkey or goat serum at 37 °C for 1 h, followed by overnight incubation at 4 °C with primary antibodies: guinea pig anti-TRPV1 (1:200, ACC-030-GP, Alomone), rabbit anti-p-CamkII*α* (1:400, ab5683, Abcam), rabbit anti-p-CREB (1:400, #9198 s, CST), rabbit anti-SP (1:1000, ab67006, Abcam), rabbit anti-CGRP (1:1000, #14959 s, CST), mouse anti-NeuN (1:400, GTX30773, GeneTex), mouse anti-CD11b (1:400, ab1211, Abcam), and mouse anti-GFAP (1:400, #3670 s, CST). The next day, the slides were taken out of the refrigerator, rinsed clean of primary antibodies, and incubated for one hour in a 37 °C environment using the corresponding secondary antibodies and counterstained with DAPI. The following secondary antibodies were used in this experiment: Alexa Fluor

594 donkey anti-mouse IgG (1:200, A-21203, Thermo Fisher), Alexa Fluor 488 donkey anti-rabbit IgG (1:400, A-21206, Thermo Fisher), Alexa Fluor 594 goat anti-rabbit IgG (1:400, ab150084, Abcam), and Alexa Fluor 488 goat anti-guinea pig IgG (1:200, ab150185, Abcam). Images were taken uniformly using Zeiss Structured Illumination Optical Section Microscope to generate fluorescent images. Quantification of images was performed using ImageJ software followed by data analysis. For a single-channel fluorescence picture, the gray value of each pixel represents the magnitude of the fluorescence intensity at that point and the formula for the average fluorescence intensity: Mean Gray Value = Integrated Density / Area (Shihan et al. 2021).

Statistical Analysis

GraphPad Prism 8 was used for statistical analysis. The experimental results were expressed as standard error of mean. A *T* test was employed to compare the two datasets. The one-way ANOVA was employed to conduct a one-factor test, whereas the two-way ANOVA was utilized for the two-factor test. The discrepancy was deemed statistically significant when $p < 0.05$.

Results

The Establishment of the Rat DNP Model

Using known methods documented in the literature (He et al. 2023), we modeled DNP by intraperitoneal injection of STZ (Fig. 1A). The DNP model rats showed a clear decrease in BW and a remarkable in FBG levels after 7 days of STZ injection compared to control group (Fig. 1B, C). After 14 days from STZ injection, DNP rats showed obvious mechanical allodynia in the hind paw, which persisted for a minimum of 1 week (Fig. 1D). Area under the curve (AUC) analysis showed the PWT response of the rats (Fig. 1E).

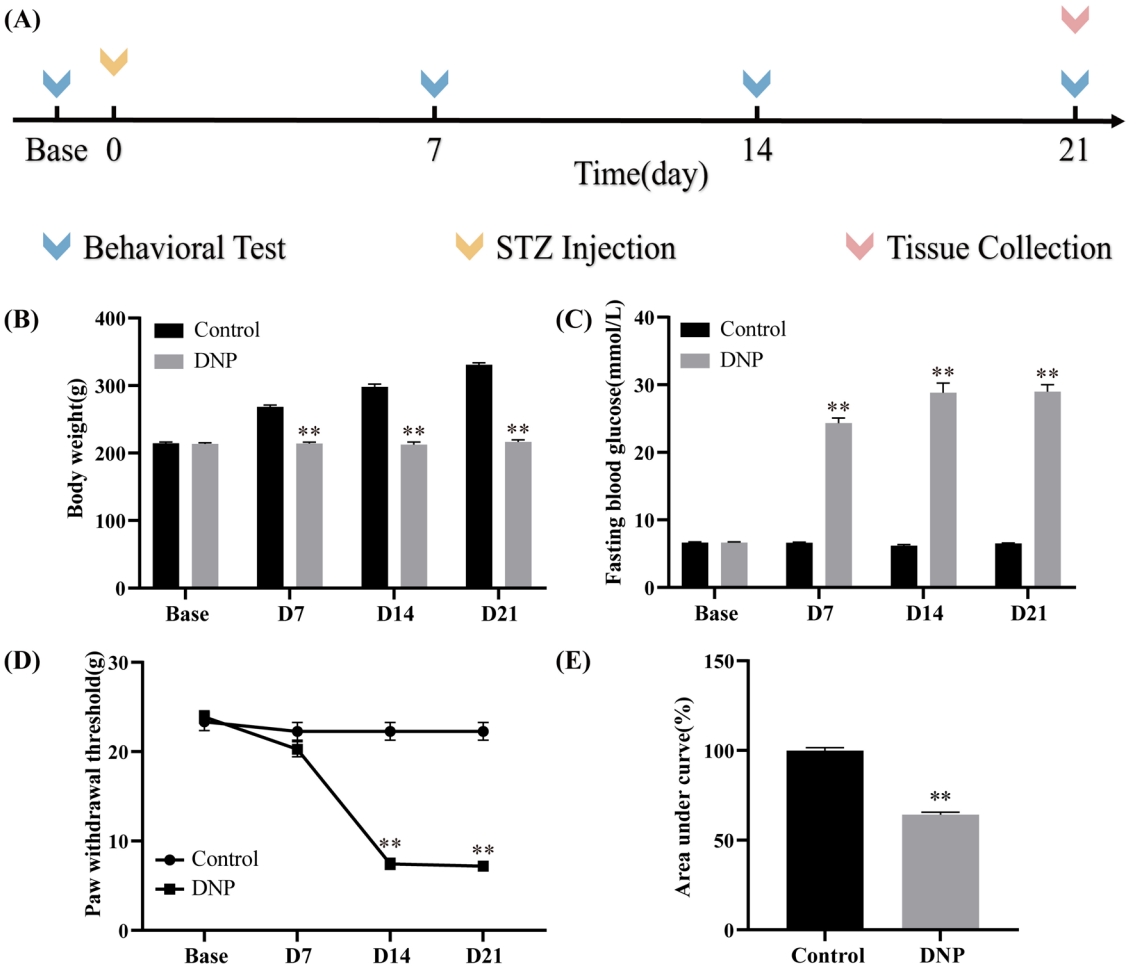

Fig. 1 Establishing the DNP model. **A** Experimental procedure for the establishment of STZ-induced DNP rat model. **B, C, D** The effects of STZ injection on BW (**B**), FBG (**C**), and PWT (**D**) in rats. **E** AUC analysis of Fig. 1D. Each group consists of 6 rats. $^{**}p < 0.01$ against control group

It was evident that the rats injected with STZ and classified as DNP rats exhibited statistically significant differences in BW, FBG, and PWT in comparison to the control group. These differences were observed from 14 to 21 days following the STZ injection, confirming the accomplished implementation of the DNP model.

TRPV1 and p-CaMKIIα Co-localize and Overexpress on SCDH in DNP Rats

We observed the upregulation in the expression of both TRPV1 and p-CaMKIIα on SCDH of DNP rats by double immunofluorescence staining (Fig. 2A–C), and there was co-localization between them (Fig. 2A, D–E). This result indicated that TRPV1 and p-CaMKIIα are both overexpressed on SCDH in DNP rats, and there might be a potential functional association between them.

TRPV1-Related Co-localization on SCDH in DNP Rats

Double immunostaining analysis demonstrated a predominant degree of co-localization of p-CaMKIIα and p-CREB with NeuN, but there was minimal co-localization with GFAP or CD11b on rat SCDH with DNP (Fig. 3). This suggests that CaMKII/CREB pathway is mostly expressed in neurons rather than astrocytes or microglia. As principal mediators of neurogenic inflammation, the co-localization of substance P (SP)/calcitonin gene-related peptide (CGRP) and TRPV1 was also detected (Fig. 4).

Role of TRPV1 in Nociceptive Behaviors and CaMKII/CREB Activation in DNP Rats

According to Fig. 2B, TRPV1 expression was elevated in DNP rats, indicating its association with mechanical allodynia. In order to further investigate this subject, we used a pharmacological approach to treat the DNP rats and observed the changes (Fig. 5A). We utilized capsazepine to investigate the effect of TRPV1 in nociceptive hypersensitivity on the SCDH in DNP rats. To start with, the DNP rat model was established based on the previous section (Fig. 5B–E). The behavioral results showed that rats in the DNP + veh group illustrated a statistically differentiated reduction in PWT compared with the control + veh group since 14 days after STZ injection. However, intrathecal injection of capsazepine for one consecutive week from 15 days after STZ injection significantly increased mechanical pain threshold and alleviated nociceptive hypersensitivity in DNP rats (Fig. 5D, E). Similarly, we used the CaMKII inhibitor KN-93 to intervene in DNP rats. The experimental results were consistent with the previous findings, and KN-93 likewise alleviated pain hypersensitivity in DNP rats

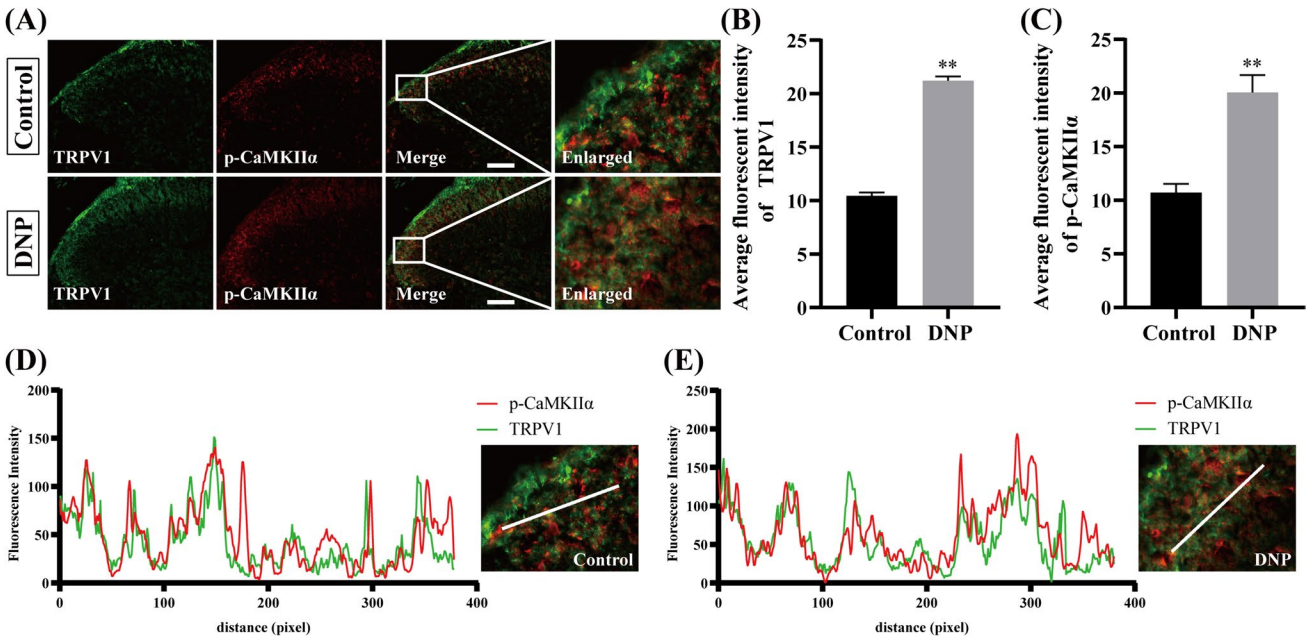

Fig. 2 Co-localization and overexpression of TRPV1 and p-CaMKII. **A** Immunofluorescence representative chart showing co-expression of TRPV1 (green) and p-CaMKIIα (red) on rat SCDH in the Control and the DNP groups. The area in the white box is enlarged on the right. **B, C** Average fluorescent intensity of TRPV1 (**B**) and p-CaMKIIα (**C**) in SCDH of rats in different groups. **D, E** Immunofluorescence representative chart showing colocalization of TRPV1 (green) and p-CaMKIIα (red) in the control (**D**) and the DNP (**E**) groups on the right. Fluorescence intensity trace plotted according to the right white line. The scale bar denotes a length of 100 μm. $n = 3$ rats each group. $^{**}p < 0.01$ against control group

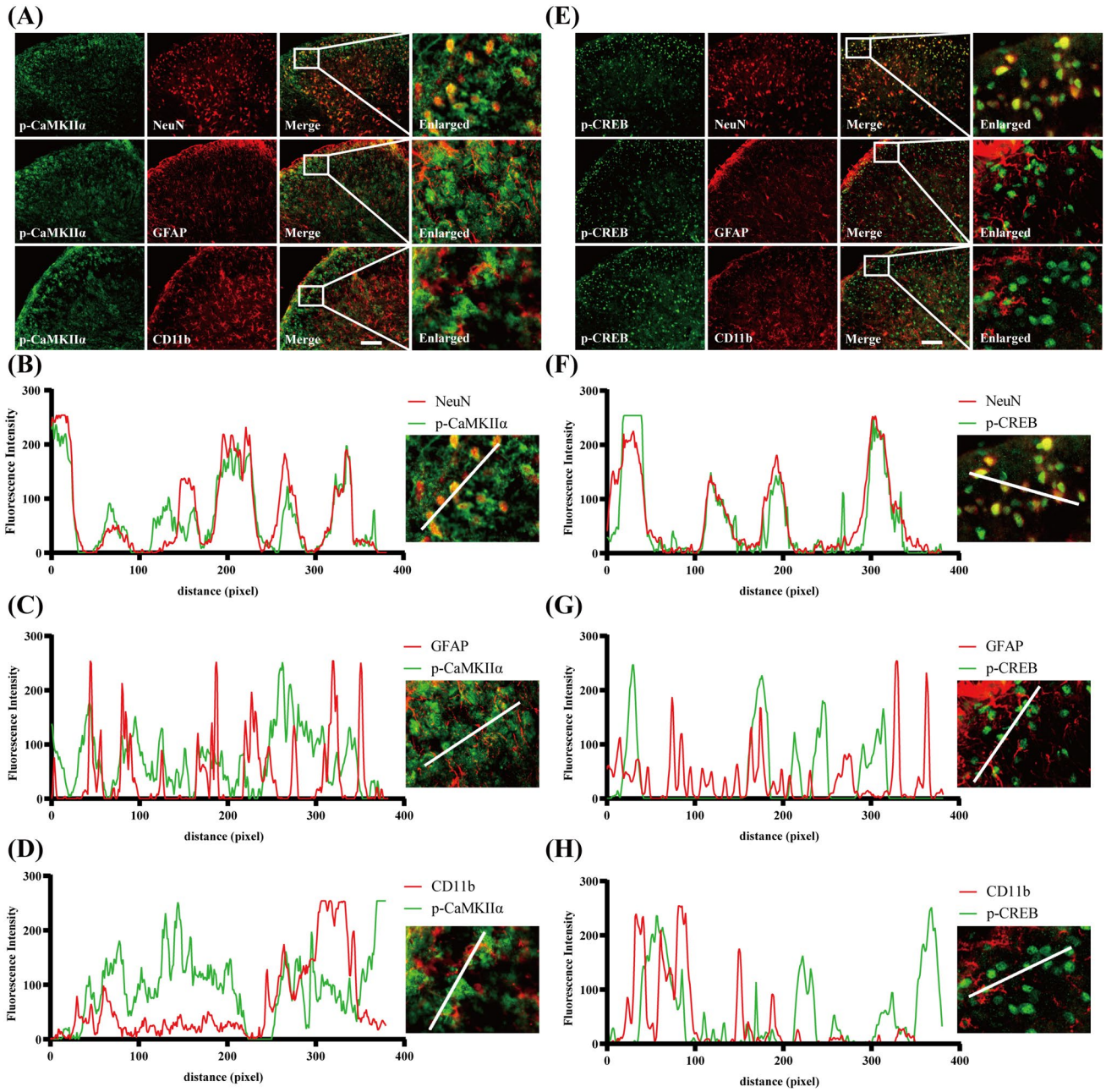

Fig. 3 Localization of phosphorylated CaMKIIα and p-CREB. **A, E** Immunofluorescence representative chart showing co-localization of p-CaMKIIα (**A**)/p-CREB (**E**) (green) and NeuN/GFAP/CD11b (red) on rat SCDH in the DNP groups. The area in the white box is enlarged on the right. **B–D** Immunofluorescence representative chart showing colocalization of p-CaMKIIα (green) and NeuN (**B**)/GFAP (**C**)/CD11b (**D**) (red) on the SCDH of DNP rat. Fluorescence intensity trace plotted according to the right white line. **F–H** Immunofluorescence representative chart showing colocalization of p-CREB (green) and NeuN (**F**)/GFAP (**G**)/CD11b (**H**) (red) on the SCDH of DNP rat. Fluorescence intensity trace plotted according to the right white line. Scale bar indicates 100 μm

(Fig. 5D, E). These results confirmed that spinal TRPV1 and CaMKII/CREB pathway played a nociceptive role in the pathological progress of DNP.

Subsequently, our investigation centered on the correlation between TRPV1 and the CaMKII/CREB pathway on SCDH. Western blot results demonstrated a notable reduction in the protein level of TRPV1 following the intrathecal administration of capsazepine, as compared with the DNP + veh group; however, no discernible disparity was noted in the protein expression of TRPV1 after the application of KN-93 (Fig. 6A, B). Meanwhile, the protein level of p-CaMKIIα was obviously downregulated with the application of both capsazepine and KN-93 compared with the DNP + veh group (Fig. 6C, E–G). The same went for

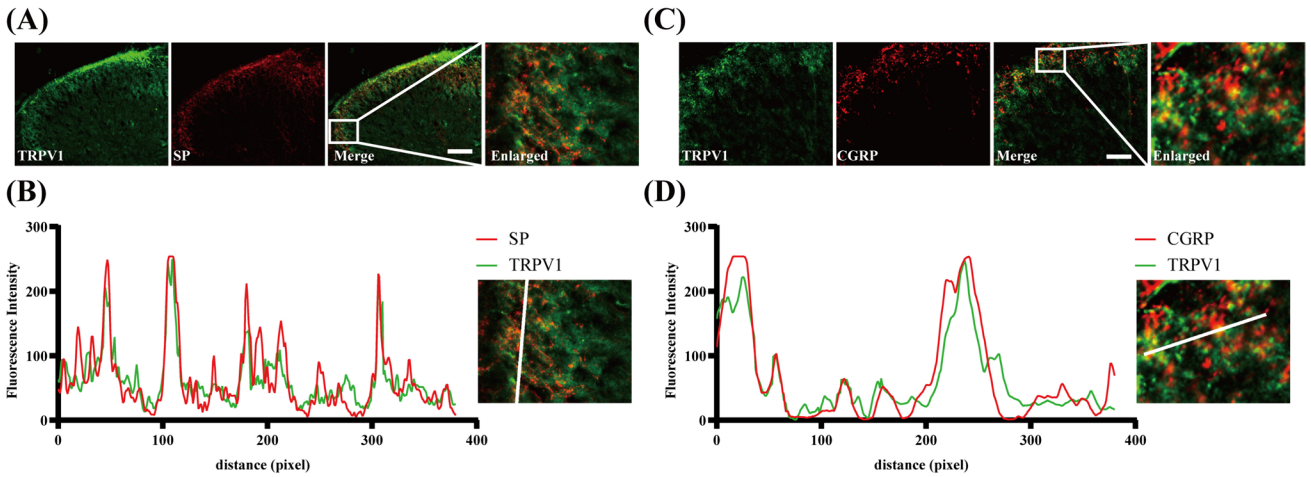

Fig. 4 Localization of TRPV1 and SP/CGRP. **A, C** Immunofluorescence representative chart showing co-localization of TRPV1 (green) and SP (**A**)/CGRP (**C**) (red) on rat SCDH in the DNP group. The area in the white box is enlarged on the right. **B, D** Immunofluorescence representative chart showing colocalization of TRPV1 (green) and SP (**B**)/CGRP (**D**) (red) on the SCDH of DNP rat. Fluorescence intensity trace plotted according to the right white line. Scale bar indicates 100 μm

p-CREB expression (Fig. 6D, H–J). The immunofluorescence results confirmed that the application of KN-93 did not influence the average fluorescence intensity of TRPV1 (Fig. 7A). However, the expression of p-CaMKIIα and p-CREB was dramatically diminished after injection of capsazepine (Fig. 7B, C). Following the administration of capsazepine and KN-93, the protein expression of tumor necrosis factor-α (TNF-α) was downregulated (Fig. 8B). Additionally, the mean fluorescence intensity of both SP and CGRP was also remarkably diminished (Fig. 8A, C). The above findings suggested the CaMKII/CREB pathway is a downstream target of TRPV1 in SCDH under DNP.

EA is Effective in Relieving DNP

We next treated the DNP rats with EA (Fig. 9A). Although EA could not reverse BW or FBG in rats with DNP (Fig. 9B, C), it resulted in a significant increase in PWT, indicating a promising analgesic effect (Fig. 9D, E). The finding aligned with the clinical outcomes, confirming the efficacy of EA (Lee et al. 2013).

EA Decreased the Expression of TRPV1 and Its Downstream Substances on SCDH in DNP Rats

Subsequently, we examined the fundamental pathways by which EA induces pain relief in DNP rats. This part of the research mainly investigated the impact of EA intervention on the activation of TRPV1 and its downstream molecules in SCDH of DNP rats. We found that regardless of protein expression or fluorescence intensity, TRPV1, p-CaMKIIα, p-CREB, TNF-α, SP, or CGRP were all noticeably increased in SCDH of DNP group compared with the control group (Figs. 10 and 11). Additionally, EA intervention significantly reversed all the overexpression (Figs. 10 and 11). These data suggested that EA effectively attenuated TRPV1 and its downstream activation in SCDH of DNP rats, indicating that TRPV1 and its downstream CaMKII/CREB pathway may be a crucial target for EA to improve DNP.

Exogenously Applied TRPV1 Agonist Capsaicin Reversed the Analgesic Effect Induced by EA

The behavioral results of the rats provided evidence for the successful creation of the DNP rat model (Fig. 12). Capsaicin, a TRPV1 agonist, was administered intrathecally to part of the EA-intervened DNP rats at a frequency of once daily for 7 days. The remaining DNP rats with EA operation were treated with the appropriate vehicles. We further explored the effect of capsaicin on the reversal of mechanical hyperalgesia by EA in DNP rats. From the comparison of the DNP + EA + capsaicin and the DNP + EA + veh group, intrathecal injection of capsaicin apparently reversed the analgesic effect induced by EA (Fig. 12D). AUC analysis showed that continuous capsaicin intervention resulted in increased mechanical allodynia (Fig. 12E). The aforementioned findings suggest pain-relieving effect induced by EA was counteracted through the intrathecal application of capsaicin, a TRPV1 agonist.

The results from both western blot and immunofluorescence suggest that capsaicin was capable of reversing the decrease in expression of p-CaMKIIα, p-CREB, TNF-α, SP, and CGRP produced by EA intervention (Figs. 13 and 14).

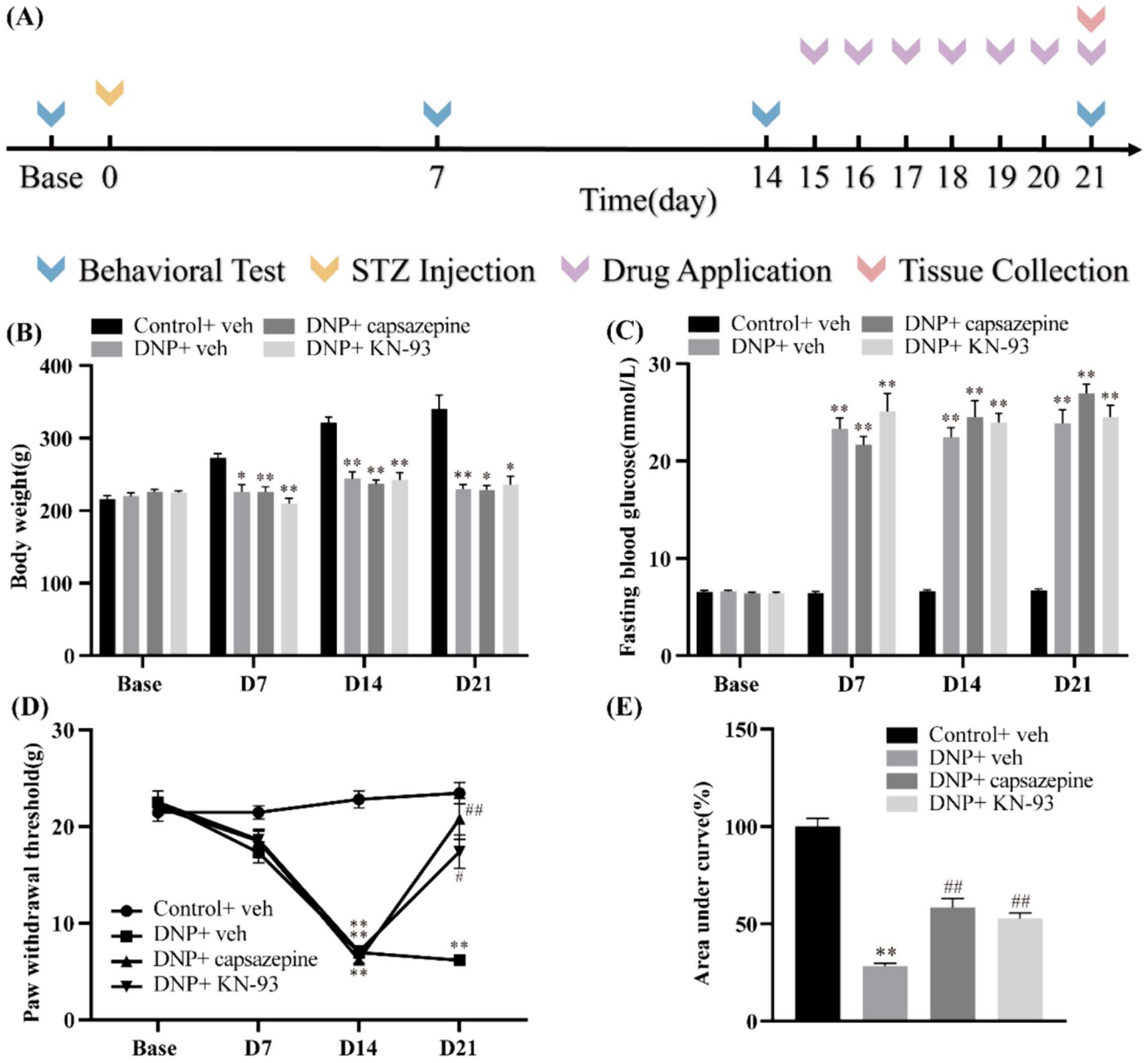

Fig. 5 Behavioral effects of intrathecal injection of capsazepine and KN-93 in DNP rats. **A** Protocols for experiments. **B–D** Effects of STZ and intrathecal drug application on BW (**B**), FBG (**C**), and PWT (**D**) in rats. **E** AUC analysis of Fig. 5D within D15-21. $n=8$. $^{*}p<0.05$, $^{**}p<0.01$ against control + veh group. $^{\#}p<0.05$, $^{\#\#}p<0.01$ against DNP + veh group

All the above results demonstrated that EA mitigates DNP by means of the TRPV1-mediated CaMKII/CREB pathway.

Discussion

Prior studies investigating the causes of DNP have mostly concentrated on changes in the excitability of peripheral sensory nerves while giving little attention to the regulation of central nociceptive sensitization. As in several previous studies by our team, all of which focused on the dorsal root ganglion, we investigated the changes of p-CaMKIIα, TRPV1, SP, and CGRP in DNP rats and probed the role of EA in the regulation of DNP (He et al. 2017, 2023; Ma et al. 2023; Li et al. 2024). Nevertheless, it is an established truth that harmful stimuli on the periphery can also induce changes in the adaptability of the central nervous system (Zhang et al. 2019). Owing to the technological advances, in technology, we have even been able to visualize significant reductions in spinal cord cross-sectional area in patients with DNP on MRI (Eaton et al. 2001). The subclinical diabetic neuropathy may cause spinal cord atrophy, indicating that

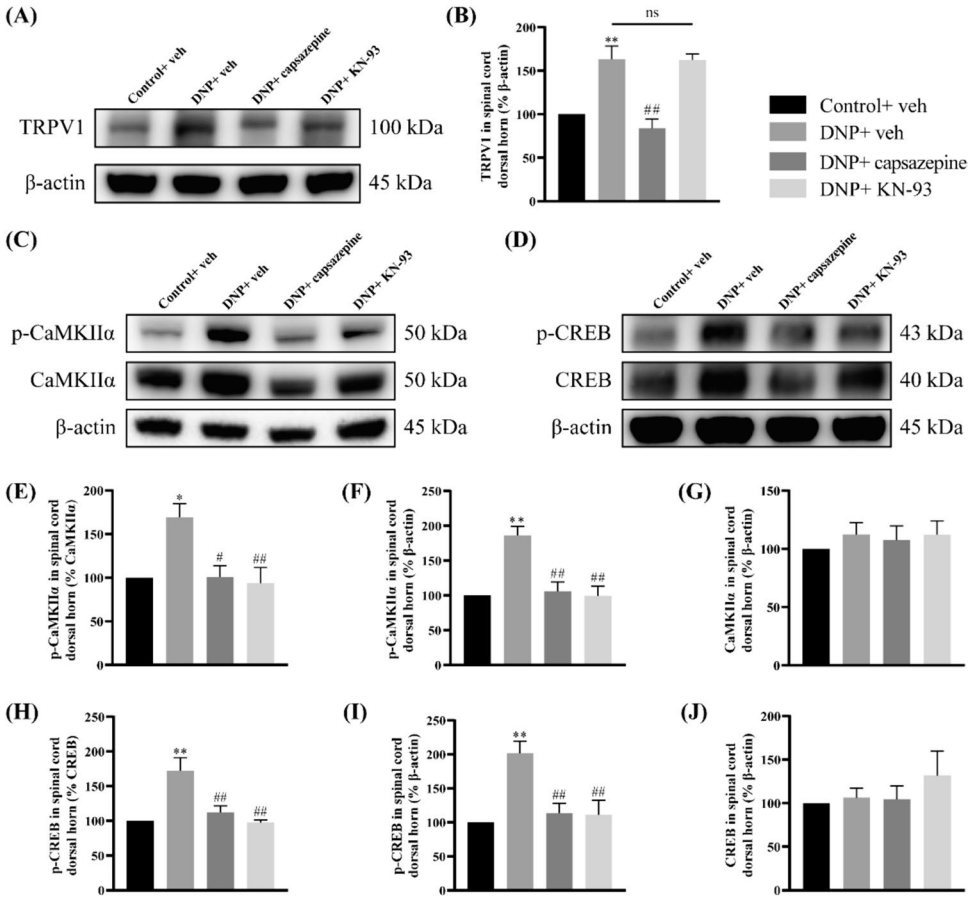

Fig. 6 Capsazepine reduced the protein level of p-CaMKIIα and p-CREB, whereas KN-93 had no effect on TRPV1. **A, C, D** Representative western blotting images of TRPV1 (**A**), p-CaMKIIα (**C**), and p-CREB (**D**). **B** Quantitative results of TRPV1. **E–G** Quantitative results of p-CaMKIIα. **H–J** Quantitative results of p-CREB. β-Actin was used as a reference control. There are 5 rats in each group. $^{*}p<0.05$, $^{**}p<0.01$ against Control + veh group. $^{\#}p<0.05$, $^{\#\#}p<0.01$ against DNP + veh group

central changes may occur before peripheral nerve injury (Selvarajah et al. 2006). The findings in our report also indicated the presence of central alterations in DNP, with STZ-induced DNP rats having elevated expression of TRPV1 and its downstream CaMKII/CREB pathway on the SCDH compared to the control group.

TRPV1 is found in sensory neurons involved in pain perception, as well as in C- and Aδ fibers, which may contain different neuropeptides including SP and CGRP (Julius 2013). The release of neuropeptides causes the action potential to be generated that transduces signals to the central nervous system, ultimately leading to the perception of pain (Holzer and Izzo 2014). As can be found in the results of this study, SP and CGRP expressions are elevated on SCDH in DNP rats. However, EA treatment can reverse this increased activity. Moreover, TRPV1 inhibitors decrease the expression of SP and CGRP, while TRPV1 agonists promote their expression. Additionally, TRPV1 activation additionally results in the release of inflammatory substances into the periphery (Sintsova et al. 2021).

Capsaicin, the active constituent of chili peppers, selectively activates TRPV1 and produces intense burning pain. Similar to the aforementioned experimental findings, we found that intrathecal injection of capsaicin resulted in a prominent downregulation in PWT, indicating enhanced pain sensitivity of rats with DNP. Paradoxically, capsaicin is widely used as an analgesic in therapeutic settings. There is also a wide range of studies addressing this issue. Research findings have demonstrated that capsaicin caused mechanical abnormal pain and thermal sensitization pain (Li et al. 2019), which is consistent with our results. TRPV1 is seen to co-localize with SP and CGRP in Fig. 1, just as another study demonstrated that TRPV1 and SP/CGRP jointly mediate pain (Wick et al. 2006). Following the tissue's exposure to a harmful stimulus, the release of SP and CGRP, which are the main triggers of neurogenic inflammation, initiated a series of inflammatory signals, resulting in the development of edema and the sensation of pain (Cianchetti 2010). The capsaicin stimulation may ablate sensory neurons, leading to long-term desensitization, and is accompanied by irreversible depletion of SP and CGRP, resulting in an analgesic effect (Nathan et al. 2002).

TNF-α is a cellular factor that promotes inflammation and has a major contribution to inflammatory and neuropathic pain (Clark et al. 2013). Research indicates that the interaction of TNF-α and TRPV1 leads to regulation of ion channel function and protein expression in neuropathic pain (Leo et al. 2017). As shown in the results,

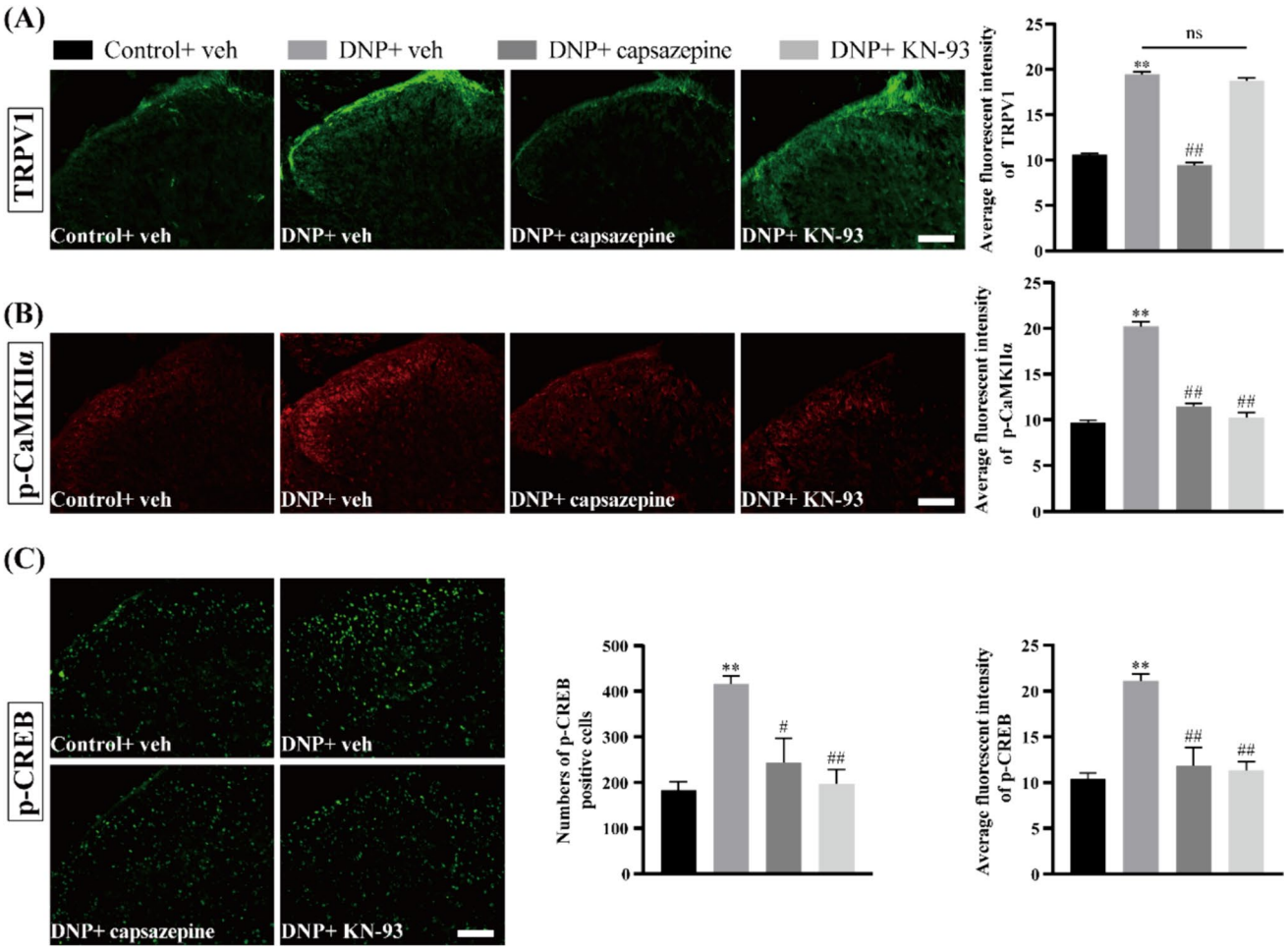

Fig. 7 Capsazepine downregulated the fluorescence intensity of p-CaMKIIα and p-CREB, whereas KN-93 had no effect on TRPV1. Immunostaining pictures and average fluorescence intensity showing the effect of capsazepine/KN-93 application on TRPV1 (**A**), p-CaMKIIα (**B**), and p-CREB (**C**). There are three rats in each group. $^{**}p < 0.01$ against control + veh group. $^{\#}p < 0.05$, $^{\#\#}p < 0.01$ against DNP + veh group. The scale bar denotes a length of 100 μm

TNF-α protein expression is elevated on SCDH in DNP rats, which is reversed by EA. TRPV1 inhibitors decrease the protein expression of TNF-α, while TRPV1 agonists do the opposite.

Calcium binding to CaMKII results in autophosphorylation on the Thr286 site (Morris and Török 2001). The outcomes of several reports showed that the increase in the alpha isoform of phosphorylated CaMKII is one of the main forms that exhibit the degree of correlation with DNP (Ferhatovic et al. 2013). Activated CaMKII phosphorylates CREB, binds to certain regions on target genes which is responsive to cAMP, and recruits RNA polymerase II to form a transcriptional complex that regulates transcription of target genes. As a result of increased calcium inward flow induced by nociception, phosphorylated CREB combines synaptic activity with long-term alterations in synaptic plasticity. This is considered a key response mediating the initiation and maintenance of central sensitization (Gu et al. 2010; Chen et al. 2014). The proinflammatory factor TNF-α may induce long-term synaptic plasticity by correlating with the phosphorylation levels of CREB in superficial SCDH neurons, possibly through CREB-mediated gene transcription. The findings demonstrated TRPV1 co-localized with p-CaMKIIα on the SCDH of rats with DNP. TRPV1 inhibitor capsazepine improved the nociceptive hypersensitivity and downregulated the expression of p-CaMKIIα in the DNP model rats, while CaMKII inhibitor KN-93 had no effect on TRPV1 expression. These findings indicated that the CaMKII/CREB pathway on SCDH is located downstream of TRPV1 and is regulated by TRPV1. Our study findings align with previous research validating the mediation of the CaMKII/CREB pathway by TRPV1. It has been reported that an inflammatory acidic environment activates TRPV1, leading to upregulation of CGRP expression through the CaMK-CREB cascade (Nakanishi et al. 2010). Another study showed that paeoniflorin protects diabetic mice from

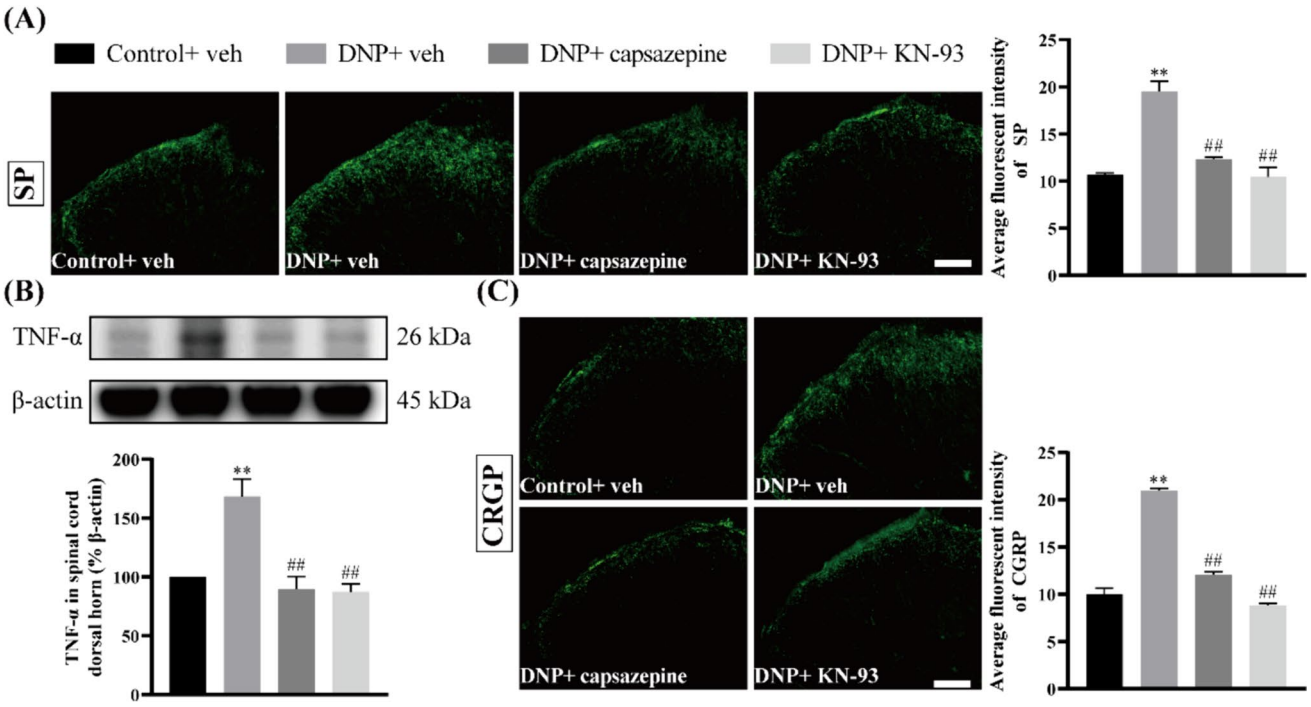

Fig. 8 Changes of pro-inflammatory pain mediators SP, CGRP, and TNF-α on various groups of rats. **A** Immunostaining pictures and average fluorescence intensity showing the effect of capsazepine/KN-93 application on SP ($n=3$). **B** The top panel is representative of western blot and the bottom one showing its protein expression statistics of TNF-α. β-Actin was used as a reference control. There were 5 rats each group. **C** Immunostaining pictures and average fluorescence intensity showing the effect of capsazepine/KN-93 application on CGRP ($n=3$). Scale bar indicates 100 μm. $^{**}p<0.01$ against control + veh group. $^{\#\#}p<0.01$ against DNP + veh group

myocardial infarction-induced heart damage through the TRPV1/CaMK/CREB signaling pathway (Han et al. 2016). It has also been shown that TRPV1 may play an important role in morphine self-administration by activating the CaMKII-CREB pathway in nucleus accumbens (Ma et al. 2018).

EA has gained global recognition as an effective treatment for various types of clinical pain. The therapeutic role of EA in DNP has also been widely demonstrated (Cho and Kim 2021), although the underlying analgesic mechanisms remain elusive. The experimental results demonstrated that EA reversed the increased sensitivity to pain induced by DNP and downregulated the overexpression of TRPV1 and its downstream CaMKII/CREB pathway. One research reported that EA suppresses TLR4 signaling and TRPV1 upregulation, leading to the relief of peripheral neuropathic pain (Li et al. 2019). Another study showed that EA produces analgesic effects on cervical spondylotic radiculopathy via suppressing the CaMKII/CREB pathway. Nevertheless, it remains uncertain if this implies that TRPV1 and its subsequent CaMKII/CREB pathway serve as the mechanism through which EA enhances nociceptive sensitivity. Therefore, to demonstrate that EA is ameliorating DNP via the TRPV1-mediated CaMKII/CREB pathway, we conducted additional verification using capsaicin. The application of TRPV1 agonist capsaicin reversed the analgesic action of EA upon restoration of its downregulated expression. By considering all these findings collectively, we identified a potential target for analgesia and demonstrated that EA alleviates DNP through the TRPV1-mediated CaMKII/CREB pathway, thus providing new insight into the clinical treatment for DNP.

Conclusions

The CaMKII/CREB pathway on SCDH is located downstream of TRPV1 and is affected by TRPV1. EA alleviated nociceptive hypersensitivity and downregulated the expression of TRPV1, p-CaMKIIα, and p-CREB in DNP rats. Intrathecal injection of capsaicin, on the other hand, reversed the above effects of EA. Collectively, these results suggest that EA alleviates DNP through the TRPV1-mediated CaMKII/CREB pathway.

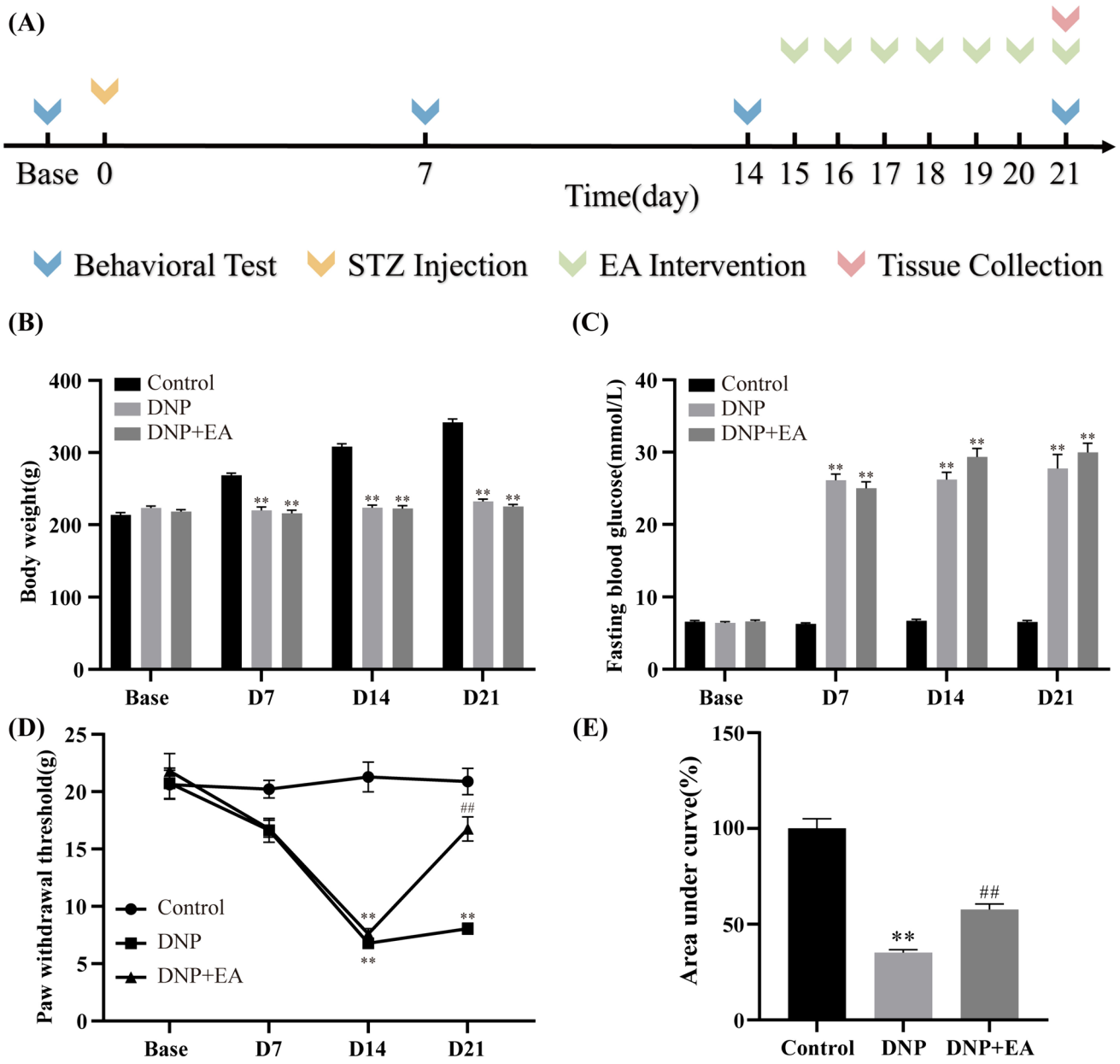

Fig. 9 EA reduced the allodynia in DNP rats. **A** Timeline for experiment. **B–D** Effects of EA intervention on BW (**B**), FBG (**C**), and PWT (**D**) in rats. **E** AUC analysis of Fig. 9D within D15-21. There were 8 rats each group. $^{**}p < 0.01$ against control group. $^{\#\#}p < 0.01$ against DNP group

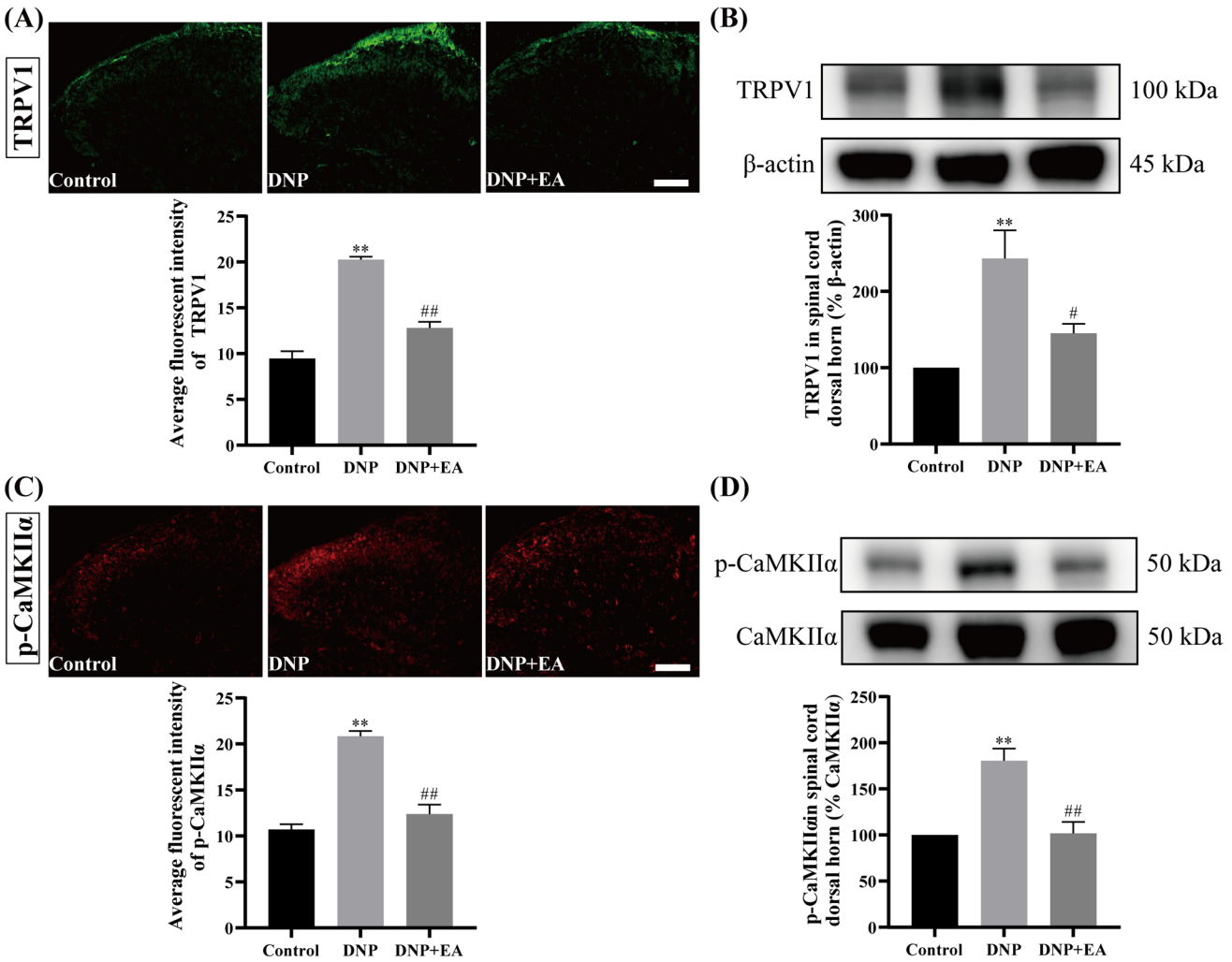

Fig. 10 EA reduces the expression of TRPV1 and p-CaMKIIα. **A, C** Immunostaining pictures and average fluorescence intensity showing the effect of EA intervention on TRPV1 (**A**) and p-CaMKIIα (**C**). There are three individuals in each group. **B, D** The top panels are representative of western blot, and the bottom ones show the protein expression statistics of TRPV1 (**B**) and p-CaMKIIα (**D**). There are 5 individuals in each group. $^{**}p < 0.01$ against control + veh group. $^{\#}p < 0.05$, $^{\#\#}p < 0.01$ against DNP + veh group. The scale bar denotes a length of 100 μm

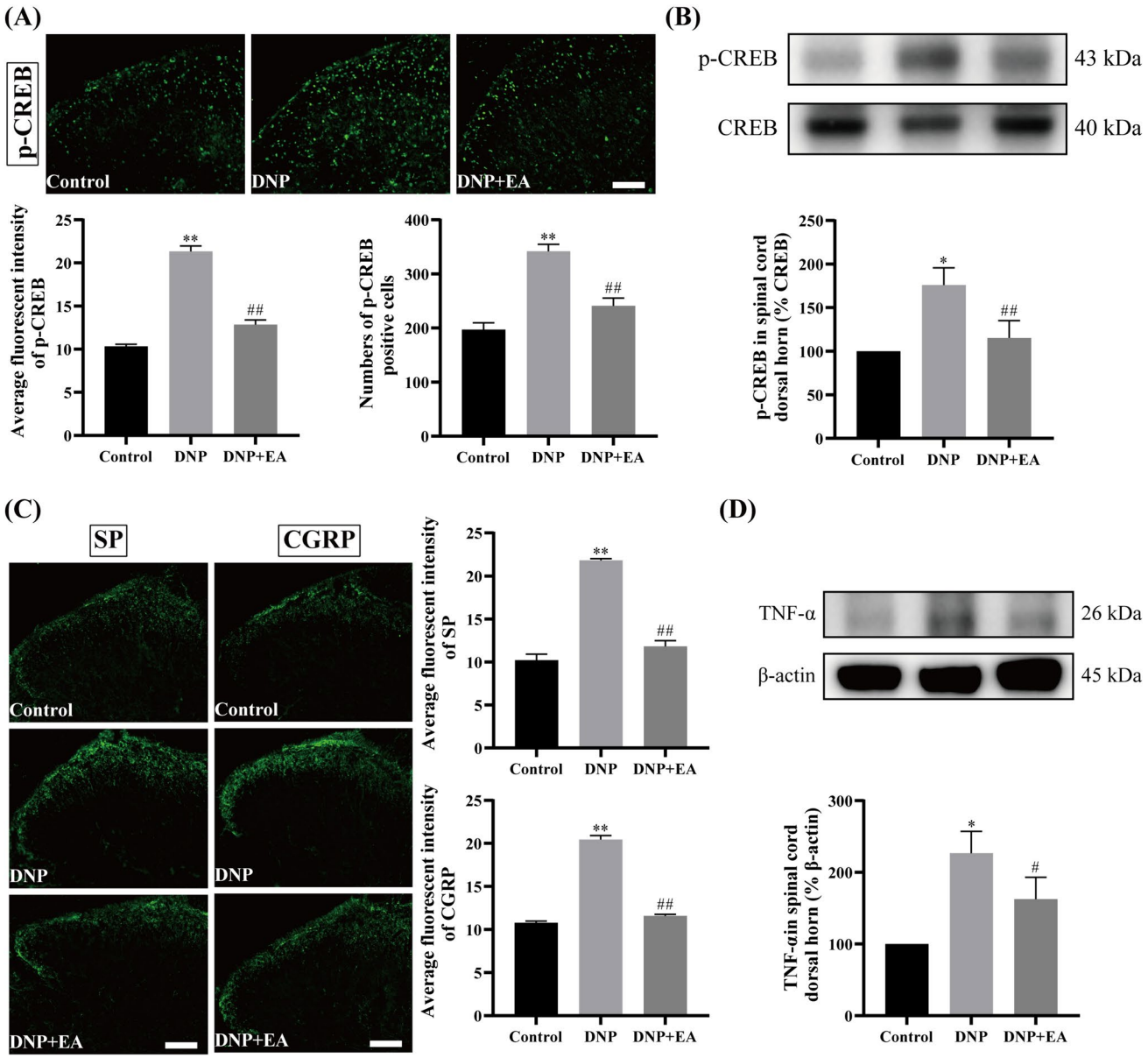

Fig. 11 EA suppresses the levels of p-CREB, SP, CGRP, and TNF-α. **A, C** Immunostaining pictures and average fluorescence intensity showing the effect of EA intervention on p-CREB (**A**), SP and CGRP (**C**). There are three individuals in each group. **B, D** The top graph is representative of western blotting and the bottom one showing its protein expression statistics of p-CREB (**B**) and TNF-α (**D**). There are 5 individuals in each group. $^{*}p<0.05$, $^{**}p<0.01$ against control + veh group. $^{\#}p<0.05$, $^{\#\#}p<0.01$ against DNP + veh group. The scale bar denotes a length of 100 μm

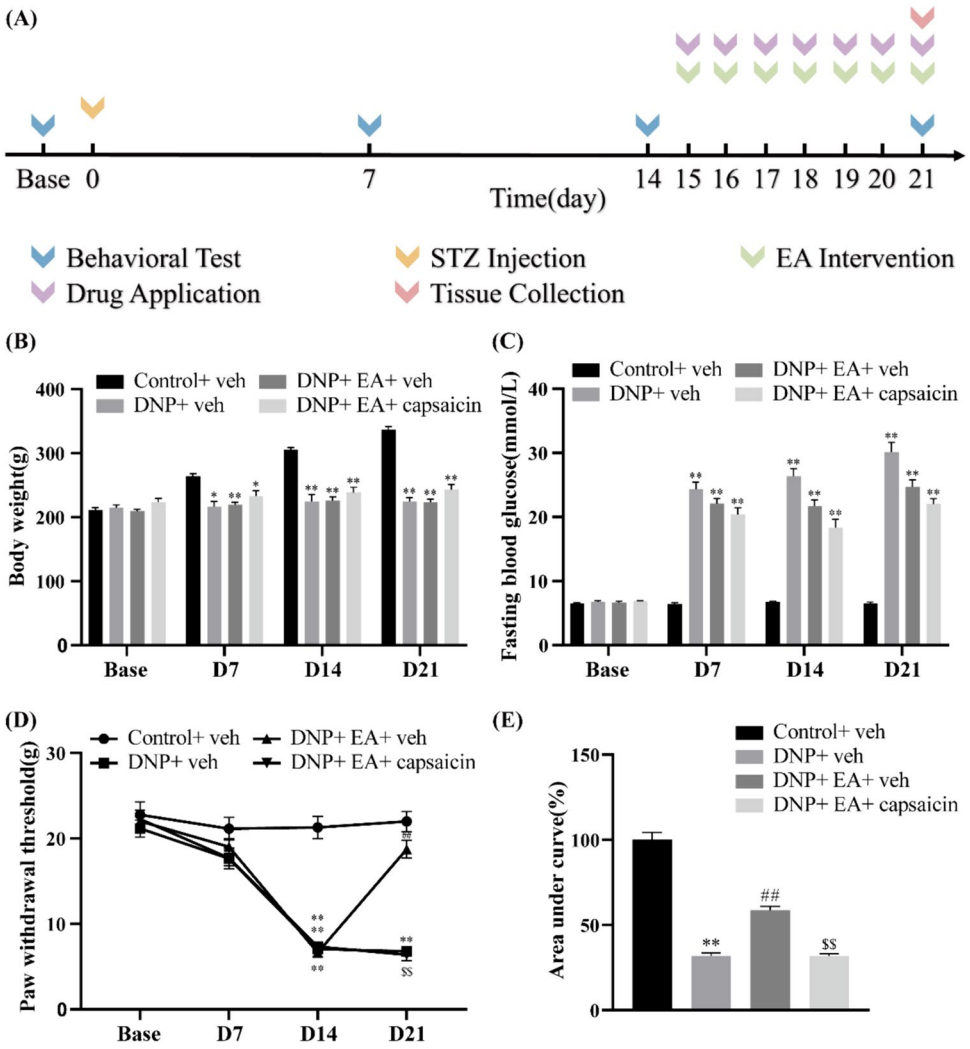

Fig. 12 Capsaicin reversed EA's analgesic effect. **A** Experimental protocol for the capsaicin application and EA intervention on DNP rats. **B–D** Effects of capsaicin application and EA intervention on BW (**B**), FBG (**C**), and PWT (**D**) in rats. **E** AUC analysis of Fig. 12D within D15-21. There are 8 rats in each group. $^{*}p < 0.05$, $^{**}p < 0.01$ against control + veh group. $^{\#\#}p < 0.01$ against DNP + veh group. $^{\$\$}p < 0.01$ against DNP + EA + veh group

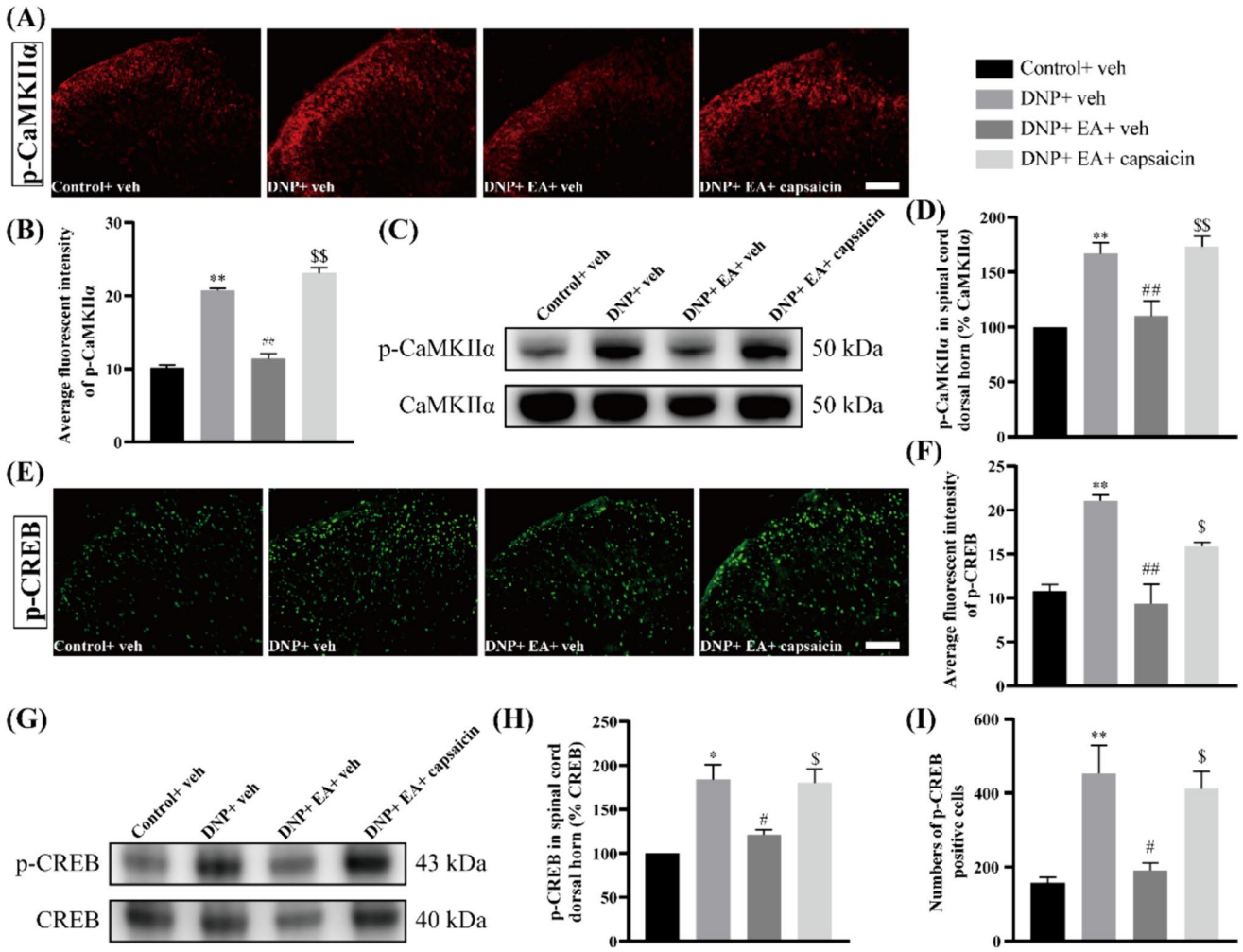

Fig. 13 Capsaicin reversed the downregulation of p-CaMKIIα and p-CREB by EA. **A** Representative immunostaining images of p-CaMKIIα. **B** Average fluorescence intensity of Fig. 13A. There are 3 rats per group. **C** Illustrative western blot images of p-CaMKIIα. **D** The summarized data of Fig. 13C. ($n=5$). **E** Representative immunostaining images of p-CREB. **F** Average fluorescence intensity of Fig. 13E. $n=3$ each group. **G** Illustrative western blot images of p-CREB. **H** The summarized data of Fig. 13G. ($n=5$). **I** Numbers of positive cells of Fig. 13E. ($n=3$). Scale bar indicates a length of 100 μm. $^{*}p<0.05$, $^{**}p<0.01$ against control + veh group. $^{\#}p<0.05$, $^{\#\#}p<0.01$ against DNP + veh group. $^{\$}p<0.05$, $^{\$\$}p<0.01$ against DNP + EA + veh group

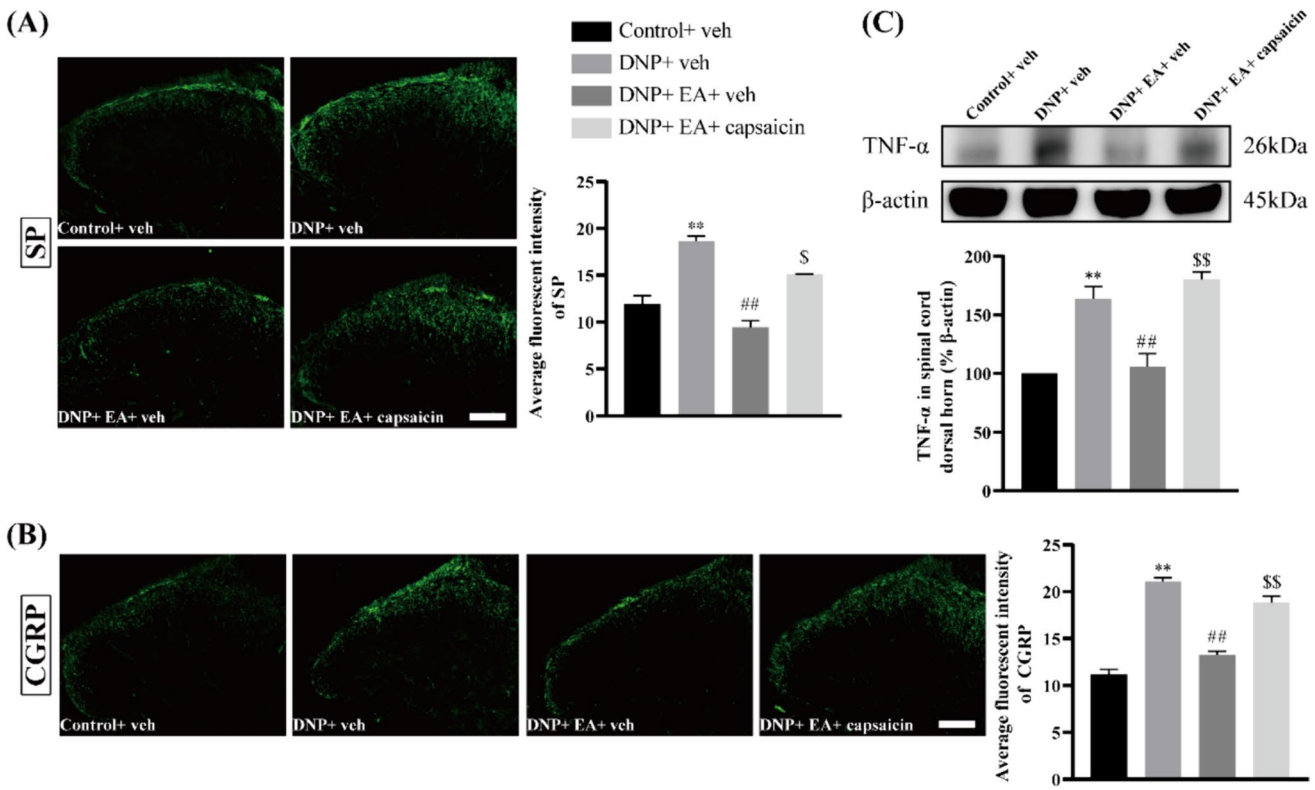

Fig. 14 Capsaicin reversed the downregulation of SP, CGRP, and TNF-α by EA. **A, B** Representative immunostaining images and average fluorescence intensity of SP (**A**) and CGRP (**B**). ($n=3$). (**C**) The top panel is representative of western blotting and the bottom one showing its protein expression statistics of TNF-α. ($n=5$). $^{**}p<0.01$ against control + veh group. $^{\#\#}p<0.01$ against DNP + veh group. $^{\$}p<0.05$, $^{\$\$}p<0.01$ against DNP + EA + veh group. Scale bar indicates a length of 100 μm

Author Contribution The original draft of the manuscript was written by Yinmu Zheng. Chi Xu oversaw the editing and review. Yinmu Zheng, Yurong Kang, Siyi Li, and Yu Zheng contributed to formal analysis. Visualization was handled by Yinmu Zheng, Yurong Kang, and Qunqi Hu. Investigation was performed by Xiaoxiang Wang, Hengyu Chi, Keying Guo, Minjian Jiang, and Zhouyuan Wei. Xiaomei Shao, Boyu Liu, Junying Du, and Xiaofen He contributed to methodology. Yongliang Jiang, Zhenzhong Lu, and Jianqiao Fang contributed to conceptualization.

Funding This work was supported by the Natural Science Foundation of Zhejiang Province of China (LY22H270006 and ZCLY24H2701), the Research Fund for Zhejiang Chinese Medical University Affiliated Hospital (2022FSYYZZ09), Jinhua Traditional Chinese Medicine Science and Technology Program (2024ZD04), and State Administration of Traditional Chinese Medicine Science and Technology Department-Zhejiang Province Co-construction Project Key Projects (GZY-ZJ-KJ-24073).

Data Availability The datasets used and analyzed during the current study are available from the corresponding author upon reasonable request.

Declarations

Ethics Approval and Consent to Participate This animal study was approved by the Animal Ethics Committee of Zhejiang Chinese Medical University, with the approval number IACUC-20190805–04.

Competing Interests The authors declare no competing interests.

References

Bach FW, Yaksh TL (1995) Release of beta-endorphin immunoreactivity into ventriculo-cisternal perfusate by lumbar intrathecal capsaicin in the rat. Brain Res 701(1–2):192–200. https://doi.org/10.1016/0006-8993(95)01003-1

Chaplan SR, Bach FW, Pogrel JW, Chung JM, Yaksh TL (1994) Quantitative assessment of tactile allodynia in the rat paw. J Neurosci Methods 53(1):55–63. https://doi.org/10.1016/0165-0270(94)90144-9

Chen S-R, Hu Y-M, Chen H, Pan H-L (2014) Calcineurin inhibitor induces pain hypersensitivity by potentiating pre- and

postsynaptic NMDA receptor activity in spinal cords. J Physiol 592(1):215–227. https://doi.org/10.1113/jphysiol.2013.263814
Cho E, Kim W (2021) Effect of acupuncture on diabetic neuropathy: a narrative review. Int J Mol Sci 22(16):8575. https://doi.org/10.3390/ijms22168575
Cianchetti C (2010) Capsaicin jelly against migraine pain. Int J Clin Pract 64(4):457–459. https://doi.org/10.1111/j.1742-1241.2009.02294.x
Clark AK, Old EA, Malcangio M (2013) Neuropathic pain and cytokines: current perspectives. J Pain Res 6:803–814. https://doi.org/10.2147/JPR.S53660
Dan Z, Tesfaye S, Spallone V, Gurieva I, Al Kaabi J, Mankovsky B, Martinka E, Radulian G, Nguyen KT, Stirban AO, Tankova T (2022) Screening, diagnosis and management of diabetic sensorimotor polyneuropathy in clinical practice: international expert consensus recommendations. Diabetes Res Clin Pract 186. https://doi.org/10.1016/j.diabres.2021.109063
Eaton SE, Harris ND, Rajbhandari SM, Greenwood P, Wilkinson ID, Ward JD, Griffiths PD, Tesfaye S (2001) Spinal-cord involvement in diabetic peripheral neuropathy. Lancet 358(9275):35–36. https://doi.org/10.1016/S0140-6736(00)05268-5
Fei X, He X, Tai Z, Wang H, Qu S, Chen L, Hu Q, Fang J, Jiang Y (2020) Electroacupuncture alleviates diabetic neuropathic pain in rats by suppressing P2X3 receptor expression in dorsal root ganglia. Purinergic Signal 16(4):491–502. https://doi.org/10.1007/s11302-020-09728-9
Ferhatovic L, Banozic A, Kostic S, Kurir TT, Novak A, Vrdoljak L, Heffer M, Sapunar D, Puljak L (2013) Expression of calcium/calmodulin-dependent protein kinase II and pain-related behavior in rat models of type 1 and type 2 diabetes. Anesth Analg 116(3):712–721. https://doi.org/10.1213/ANE.0b013e318279b540
Gu X, Zhang J, Ma Z, Wang J, Zhou X, Jin Y, Xia X, Gao Q, Mei F (2010) The role of N-methyl-D-aspartate receptor subunit NR2B in spinal cord in cancer pain. Eur J Pain 14(5):496–502. https://doi.org/10.1016/j.ejpain.2009.09.001
Han F, Zhou D, Yin X, Sun Z, Han J, Ye L, Zhao W, Zhang Y, Wang Z, Zheng L (2016) Paeoniflorin protects diabetic mice against myocardial ischemic injury via the transient receptor potential vanilloid 1/calcitonin gene-related peptide pathway. Cell Biosci 6:37. https://doi.org/10.1186/s13578-016-0085-7
Haranishi Y, Hara K, Terada T (2021) Inhibitory effect of intrathecally administered AM404, an endocannabinoid reuptake inhibitor, on neuropathic pain in a rat chronic constriction injury model. Pharmacol Rep 73(3):820–827. https://doi.org/10.1007/s43440-021-00250-2
He X-F, Wei J-J, Shou S-Y, Fang J-Q, Jiang Y-L (2017) Effects of electroacupuncture at 2 and 100 Hz on rat type 2 diabetic neuropathic pain and hyperalgesia-related protein expression in the dorsal root ganglion. J Zhejiang Univ Sci B 18(3):239–248. https://doi.org/10.1631/jzus.B1600247
He X, Kang Y, Fei X, Chen L, Li X, Ma Y, Hu Q, Qu S, Wang H, Shao X, Liu B, Du Yi-Liang, J-Y, Fang J, Jiang Y (2023) Inhibition of phosphorylated calcium/calmodulin-dependent protein kinase IIα relieves streptozotocin-induced diabetic neuropathic pain through regulation of P2X3 receptor in dorsal root ganglia. Purinergic Signal 19(1):99–111. https://doi.org/10.1007/s11302-021-09829-z
Holzer P, Izzo AA (2014) The pharmacology of TRP channels. Br J Pharmacol 171(10):2469–2473. https://doi.org/10.1111/bph.12723
Iftinca M, Defaye M, Altier C (2021) TRPV1-targeted drugs in development for human pain conditions. Drugs 81(1):7–27. https://doi.org/10.1007/s40265-020-01429-2
Julius D (2013) TRP channels and pain. Annu Rev Cell Dev Biol 29:355–384. https://doi.org/10.1146/annurev-cellbio-101011-155833
Lam WL, Wang J, Yeung WF, Cheung CW, Chan KKL, Ngan HYS, Wong CKH, Jiang F, Ma PWS, Leung TW, Leung WC, Liu TC, Chen H, Lao L (2022) A combination of electroacupuncture and auricular acupuncture for postoperative pain after abdominal surgery for gynaecological diseases: a randomized controlled trial. Phytomedicine 104:154292. https://doi.org/10.1016/j.phymed.2022.154292
Lee S, Kim J-H, Shin K-M, Kim J-E, Kim T-H, Kang K-W, Lee M, Jung S-Y, Shin M-S, Kim A-R, Park H-J, Hong K-E, Choi S-M (2013) Electroacupuncture to treat painful diabetic neuropathy: study protocol for a three-armed, randomized, controlled pilot trial. Trials 14:225. https://doi.org/10.1186/1745-6215-14-225
Leo M, Schulte M, Schmitt L-I, Schäfers M, Kleinschnitz C, Hagenacker T (2017) Intrathecal resiniferatoxin modulates TRPV1 in DRG neurons and reduces TNF-induced pain-related behavior. Mediators Inflamm 2017:2786427. https://doi.org/10.1155/2017/2786427
Li Y, Yin C, Li X, Liu B, Wang J, Zheng X, Shao X, Liang Y, Du J, Fang J, Liu B (2019) Electroacupuncture alleviates paclitaxel-induced peripheral neuropathic pain in rats via suppressing TLR4 signaling and TRPV1 upregulation in sensory neurons. Int J Mol Sci 20(23):5917. https://doi.org/10.3390/ijms20235917
Li S, Zheng Y, Kang Y, He X, Zheng Y, Jiang M, Xu X, Ma L, Wang X, Zhang K, Shao X, Fang J, Jiang Y (2024) Electroacupuncture alleviates streptozotocin-induced diabetic neuropathic pain via suppressing phosphorylated CaMKIIα in rats. NeuroReport 35(4):258–268. https://doi.org/10.1097/WNR.0000000000002000
Lu J, Yang L, Xu Y, Ai L, Chen J, Xiong F, Hu L, Chen H, Liu J, Yan X, Huang H, Chen L, Yu C (2021) The modulatory effect of motor cortex astrocytes on diabetic neuropathic pain. J Neurosci 41(24):5287–5302. https://doi.org/10.1523/JNEUROSCI.2566-20.2021
Lv Z, Xu X, Sun Z, Yang YX, Guo H, Li J, Sun K, Wu R, Xu J, Jiang Q, Ikegawa S, Shi D (2021) TRPV1 alleviates osteoarthritis by inhibiting M1 macrophage polarization via Ca2+/CaMKII/Nrf2 signaling pathway. Cell Death Dis 12(6):504. https://doi.org/10.1038/s41419-021-03792-8
Ma S-X, Kim H-C, Lee S-Y, Jang C-G (2018) TRPV1 modulates morphine self-administration via activation of the CaMKII-CREB pathway in the nucleus accumbens. Neurochem Int 121:1–7. https://doi.org/10.1016/j.neuint.2018.10.009
Ma Y-Q, Hu Q-Q, Kang YR, Ma L-Q, Qu S-Y, Wang H-Z, Zheng Y-M, Li S-Y, Shao X-M, Li X-Y, Hu H-T, Jiang Y-L, Fang J-Q, He X-F (2023) Electroacupuncture alleviates diabetic neuropathic pain and downregulates p-PKC and TRPV1 in dorsal root ganglions and spinal cord dorsal horn. Evid Based Complement Alternat Med 2023:3333563. https://doi.org/10.1155/2023/3333563
Magliano DJ, Boyko EJ (2021) IDF Diabetes Atlas 10th edition scientific committee, 2021 IDF DIABETES ATLAS 10 International Diabetes Federation Brussels
Mestre C, Pélissier T, Fialip J, Wilcox G, Eschalier A (1994) A method to perform direct transcutaneous intrathecal injection in rats. J Pharmacol Toxicol Methods 32(4):197–200. https://doi.org/10.1016/1056-8719(94)90087-6
Mixcoatl-Zecuatl T, Jolivalt CG (2011) A spinal mechanism of action for duloxetine in a rat model of painful diabetic neuropathy. Br J Pharmacol 164(1):159–169. https://doi.org/10.1111/j.1476-5381.2011.01334.x
Moran MM, Szallasi A (2018) Targeting nociceptive transient receptor potential channels to treat chronic pain: current state of the field. Br J Pharmacol 175(12):2185–2203. https://doi.org/10.1111/bph.14044
Morris EP, Török K (2001) Oligomeric structure of alpha-calmodulin-dependent protein kinase II. J Mol Biol 308(1):1–8. https://doi.org/10.1006/jmbi.2001.4584

Nakanishi M, Hata K, Nagayama T, Sakurai T, Nishisho T, Wakabayashi H, Hiraga T, Ebisu S, Yoneda T (2010) Acid activation of Trpv1 leads to an up-regulation of calcitonin gene-related peptide expression in dorsal root ganglion neurons via the CaMK-CREB cascade: a potential mechanism of inflammatory pain. Mol Biol Cell 21(15):2568–2577. https://doi.org/10.1091/mbc.E10-01-0049

Nathan JD, Peng RY, Wang Y, McVey DC, Vigna SR, Liddle RA (2002) Primary sensory neurons: a common final pathway for inflammation in experimental pancreatitis in rats. Am J Physiol Gastrointest Liver Physiol 283(4):G938-946. https://doi.org/10.1152/ajpgi.00105.2002

Rosenberger DC, Blechschmidt V, Timmerman H, Wolff A, Treede R-D (2020) Challenges of neuropathic pain: focus on diabetic neuropathy. J Neural Transm (vienna) 127(4):589–624. https://doi.org/10.1007/s00702-020-02145-7

Selvarajah D, Wilkinson ID, Emery CJ, Harris ND, Shaw PJ, Witte DR, Griffiths PD, Tesfaye S (2006) Early involvement of the spinal cord in diabetic peripheral neuropathy. Diabetes Care 29(12):2664–2669. https://doi.org/10.2337/dc06-0650

Shihan MH, Novo SG, Le Marchand SJ, Wang Y, Duncan MK (2021) A simple method for quantitating confocal fluorescent images. Biochem Biophys Rep 25:100916. https://doi.org/10.1016/j.bbrep.2021.100916

Shirahama M, Ushio S, Egashira N, Yamamoto S, Sada H, Masuguchi K, Kawashiri T, Oishi R (2012) Inhibition of Ca2+/calmodulin-dependent protein kinase II reverses oxaliplatin-induced mechanical allodynia in rats. Mol Pain 8:26. https://doi.org/10.1186/1744-8069-8-26

Sintsova O, Gladkikh I, Klimovich A, Palikova Y, Palikov V, Styshova O, Monastyrnaya M, Dyachenko I, Kozlov S, Leychenko E (2021) TRPV1 blocker HCRG21 suppresses TNF-α production and prevents the development of edema and hypersensitivity in carrageenan-induced acute local inflammation. Biomedicines 9(7):716. https://doi.org/10.3390/biomedicines9070716

Taher MG, Mohammed MR, Al-Mahdawi MAS, Halaf NKA, Jalil AT, Alsandook T (2023) The role of protein kinases in diabetic neuropathic pain: an update review. J Diabetes Metab Disord 22(1):147–154. https://doi.org/10.1007/s40200-023-01217-1

Wick EC, Hoge SG, Grahn SW, Kim E, Divino LA, Grady EF, Bunnett NW, Kirkwood KS (2006) Transient receptor potential vanilloid 1, calcitonin gene-related peptide, and substance P mediate nociception in acute pancreatitis. Am J Physiol Gastrointest Liver Physiol 290(5):G959-969. https://doi.org/10.1152/ajpgi.00154.2005

Zhang Y-Q, Ji G-C, Wu G-C, Zhao Z-Q (2002) Excitatory amino acid receptor antagonists and electroacupuncture synergetically inhibit carrageenan-induced behavioral hyperalgesia and spinal fos expression in rats. Pain 99(3):525–535. https://doi.org/10.1016/S0304-3959(02)00268-3

Zhang Z, Ding X, Zhou Z, Qiu Z, Shi N, Zhou S, Du L, Zhu X, Wu Y, Yin X, Zhou C (2019) Sirtuin 1 alleviates diabetic neuropathic pain by regulating synaptic plasticity of spinal dorsal horn neurons. Pain 160(5):1082–1092. https://doi.org/10.1097/j.pain.0000000000001489

Zhang X-M, Lun M-H, Du W, Ma F, Huang Z-Q (2022a) The κ-opioid receptor agonist U50488H ameliorates neuropathic pain through the Ca2+/CaMKII/CREB pathway in rats. J Inflamm Res 15:3039–3051. https://doi.org/10.2147/JIR.S327234

Zhang Y, Wang Y, Zhao W, Li L, Li L, Sun Y, Shao J, Ren X, Zang W, Cao J (2022b) Role of spinal RIP3 in inflammatory pain and electroacupuncture-mediated analgesic effect in mice. Life Sci 306:120839. https://doi.org/10.1016/j.lfs.2022.120839